Department of Pesticide Regulation

Brian R. Leahy
Director

M E M O R A N D U M

Edmund G. Brown Jr.
Governor

TO: Pamela Wofford
Environmental Program Manager I
Environmental Monitoring Branch

FROM: Frank Spurlock, Ph.D. *Original signed by*
Research Scientist III

DATE: August 25, 2015

SUBJECT: VARIABILITY IN SIMULATED CHLOROPICRIN AND 1,3-DICHLOROPROPENE VOLATILIZATION FROM HIGH DENSITY POLYETHYLENE AND TOTALLY IMPERMEABLE FILM TARPED BROADCAST APPLICATIONS.

INTRODUCTION

Spurlock (2015) recently reported estimates for means, within-field variation, and between-field variation of simulated chloropicrin (PIC) and 1,3-dichloropropene (13D) cumulative flux (emission ratio, ER = cumulative flux/applied fumigant) and discrete maximum 6 h period-mean flux density (max flux, ug m^{-2} s^{-1}) for shallow (12 inch) and deep (18 inch) bare ground broadcast applications. In that study, variation in modeled fluxes resulted from variation in soil properties used as inputs to the HYDRUS model: soil bulk density, soil water content and saturated soil-water content. Those data were obtained from 113 soil cores collected in 15 different fields from 2 field studies (Johnson and Tuli, 2013; Spurlock et al., 2013). The soil data reflected pre-application tillage and irrigation management practices used to meet fumigant label application requirements of soil tilth and water content. Those label requirements are the same regardless of whether a tarp is employed. This memo reports means, within-field coefficients of variation (CV), and between-field CVs of HYDRUS-simulated PIC and 13D ER and max flux for high density polyetheylene (PE) and totally impermeable film (TIF) broadcast applications. Here, the max flux for tarped applications are calculated from pre-tarp cut period mean fluxes determined for 6 hr air sampling periods typical of field studies, i.e. 0000 hr – 0600 hr, 0600 hr – 1200 hr, 1200 hr- 1800 hr and 1800 hr – 2400 hr. The tarped broadcast simulations here used the same soil data inputs as in the bare ground analysis (Spurlock, 2015).

The estimates of modeled variability in Spurlock (2015) yield a lower bound of the variability one could expect in commercial bare ground broadcast applications. More generally, the results provided (a) a statistical context for understanding HYDRUS-modeled fluxes, (b) a frame of reference for evaluating field-based flux data from individual studies, and (c) supporting data for use in developing stochastic flux estimates for use in exposure assessment. The results here extend to tarped PE and TIF broadcast applications.

Modeling Procedure

The modeling procedure employed here was identical to that detailed in Spurlock (2015) with 2 important differences. One was the imposition of a surface mass transfer resistance due to the presence of a tarp. The simulated tarp was present for 5 days post-application (PE) or 9 days post-application (TIF), with tarp removal at the end of those current label-required tarp-holding minimum times. The second difference was the magnitude of the diurnal fluctuation of the soil surface temperature – relative to the bare ground case - due to the tarp.

Tarp mass transfer resistance HYDRUS utilizes an "equivalent boundary layer thickness" to simulate the mass transfer resistance due to a tarp. The depth of the boundary layer determines the magnitude of the surface mass transfer resistance to volatilization. The relationship between the equivalent boundary layer depth *d* (cm) and a tarp's laboratory measured mass transfer coefficient *MTC* (cm sec^{-1}) is

$$d = \frac{D_g}{MTC}$$

Where D_g is the fumigant gas phase diffusion coefficient. Gas phase diffusion coefficients for PIC and 13D are 6515 cm^2 day^{-1} and 6886 cm^2 day^{-1}, respectively (Hilal et al., 2003a, 2003b). PIC and 13D boundary layer depths of 330 cm and 66 cm, respectively, were determined as the median depth calculated from laboratory tarp permeability data for 20 HDPE tarps (Paperniek and Yates, 2010) and used in the simulations here. Boundary layer depths of 2230 cm and 1326 cm were used to simulate the TIF tarp for PIC and 13D, respectively, based on calibrated values determined in the recent Lost Hills study. The tarp in that study was a Raven Vaporsafe™ TIF.

Soil surface temperature Fumigant transport processes are generally temperature dependent. HYDRUS typically requires specification of soil surface temperature as a boundary condition to simulate heat transport. Air temperature data are usually available for most field studies, but soil surface temperatures are not generally equal to air temperature, even for bare soil. When a tarp is present, under-tarp surface temperature depend on the tarp material. Here the under tarp surface temperatures for the TIF simulations were those measured directly in the Lost Hills study (Spurlock et al., 2013). For the PE simulations, under tarp temperatures were based on adjusting the Lost Hills air temperatures using the adjustment scheme for PE tarps detailed in Spurlock (2013).

RESULTS

Effect of tarp on flux

The effect of tarp type (bare vs PE vs TIF) on both simulated ER and max flux at both application depths was as expected from existing field and modeling studies. In general, bare ground cumulative and discrete fluxes (i.e., ER and max flux, respectively) were the highest among tarp classifications (Tables 1 and 2), while PE tarps displayed modestly lower fluxes. One exception was for 13D deep PE applications where slightly higher max flux was observed than

for the corresponding bare ground application (Table 2). That difference was within the range of numerical modeling mass balance error (generally <0.6%), and reflected the effect of differences in the soil temperature regime between PE and bare ground simulations. The low permeability TIF simulations yielded much lower fluxes for both fumigants at both depths (Tables 1 and 2). The reduction in flux for PE applications relative to bare ground was generally greater for PIC than 13D, consistent with the lower permeability of PE tarps to PIC as compared to 13D (Paperniek and Yates, 2010).

Table 1. Grand mean and between-field CVs for PIC ER and max flux. Grand mean is the mean of the 15 field means for each tarp type. The between CV is the standard deviation of the 15 field means for each tarp type divided by the grand mean. Maxflux is normalized to 100 lb acre^{-1} applied. Bare ground data from Spurlock (2015), shown here for comparison.

Surface	Depth	ER	CV (ER)	Maxflux (ug m^{-2} sec^{-1})	CV (max flux)
BARE	12”	0.528	0.18	45.2	0.43
PE	12”	0.305	0.21	17.7	0.27
TIF	12”	0.091	0.24	4.9	0.17
BARE	18”	0.329	0.40	15.4	0.56
PE	18”	0.207	0.40	12.6	0.27
TIF	18”	0.065	0.41	2.9	0.43

Table 2. Grand mean and between CV for 13D ER and max flux. Grand mean is the mean of the 15 field means for each tarp type. The between CV is the standard deviation of the 15 field means for each tarp type divided by the grand mean. Max flux is normalized to 100 lb acre^{-1} applied. Bare ground data from Spurlock (2015), shown here for comparison.

Surface	Depth	ER	CV (ER)	Maxflux (ug m^{-2} sec^{-1})	CV (max flux)
BARE	12”	0.542	0.18	33.8	0.45
PE	12”	0.456	0.23	27.8	0.37
TIF	12”	0.148	0.27	5.8	0.21
BARE	18”	0.336	0.42	12.4	0.61
PE	18”	0.291	0.45	12.5	0.54
TIF	18”	0.109	0.43	3.3	0.53

Within-field versus between field variability

The previous study of ER and max flux variability in bare ground broadcast applications evaluated the magnitude of within-field to between-field variability (Spurlock, 2015). One reason for conducting those comparisons was to understand the relative importance of within-field samples versus number of fields sampled when designing studies to estimating overall mean fluxes for specific application types. The approach taken in that study was to compare

between-field and within-field CVs for PIC and 13D ER and maxflux. The rationale for comparing CVs - as opposed to conducting analysis of variance - is discussed in Spurlock (2015). A similar analysis was conducted here for the PIC and 13D PIC simulations. Figure 1 is an example of a within versus between comparison of max flux variability based on CV comparison for a 12 inch application of PIC with PE tarp.

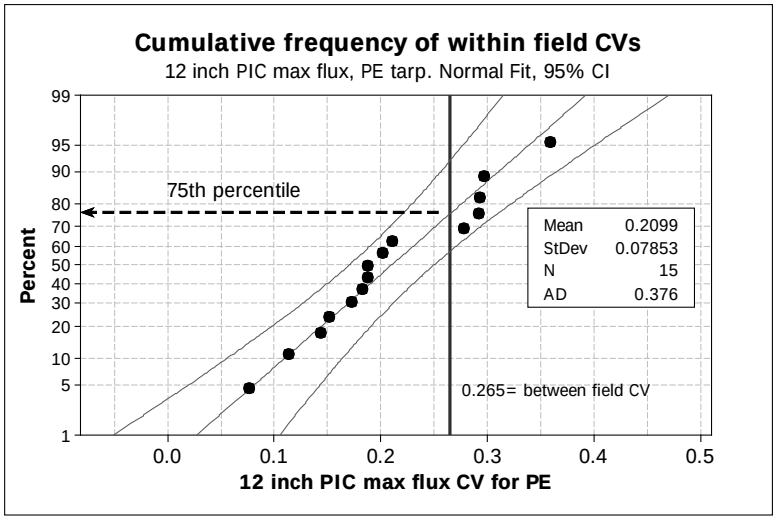

Figure 1. Comparison of within- and between-max flux CV for 12 inch PIC application with PE tarp. Max flux (ug m^{-2} sec^{-1}) expressed on 100 lbs ac^{-1} applied basis.

Similar to the bare ground scenarios, between-field variability of ER and max flux is greater than within-field variability for all modeling scenarios (Table 3). Within field ER and maxflux means and CVs are reported in Appendix 1.

Table 3. Matching percentiles of within-field CVs for the observed between-field CVs

Fumigant	tarp	12 inch ER	12 inch max flux	18 inch ER	18 inch max flux
PIC	**PE**	0.76	0.75	0.93	0.82
PIC	**TIF**	0.91	0.70	0.98	0.91
13D	**PE**	0.75	0.75	>0.99	0.98
13D	**TIF**	0.95	0.75	0.99	0.95

Distribution of max flux data

One potential use of the field mean max flux data is for generating stochastic max flux estimates for use in Monte Carlo analyses of specific application scenarios. This typically entails fitting a

distribution to the data and subsequent sampling of the fitted distribution. The 15 discrete field-mean max fluxes were adequately described by the Normal distribution based on a non-significant A-D test statistic ($\alpha = 0.05$). However, in some cases several other distributions adequately fit the data based on the A-D statistic. These included log-Normal and Weibull distributions. Therefore, a comprehensive distributional goodness-of-fit analysis should be conducted prior to Monte Carlo analysis.

CONCLUSION

Variability in ER and max flux for PE and TIF tarped broadcast applications was similar to that previously reported for bare ground application scenarios (Spurlock, 2015) in that between-field CVs for ER and max flux were:

- greatest for the deeper applications as compared to the shallow applications,
- greater for max flux than for ER in most cases, and
- greater than within-field CVs.

The between-field CVs here reflect variability arising from field-to-field differences in initial water content, soil bulk density and saturated water content. They do not reflect variation from different manufacturers or differences in tarp condition between fields that might occur due to application differences (e.g. amount of stretching or rips, if any). As such, the CVs here provide a lower bound to expected variability in actual applications.

REFERENCES

Hilal, S.H., S.W. Karickhoff and L.A. Carreira. 2003a. Prediction of Chemical Reactivity Parameters and Physical Properties of Organic Compounds from Molecular Structure using SPARC. USEPA publication 600/R-03/030. On-line: http://www.epa.gov/athens/publications/reports/EPA_600_R03_030.pdf.

Hilal, S.H., S.W. Karickhoff and L.A. Carreira. 2003b. Verification and Validation of the SPARC Model. USEPA publication 600/R-03/033. On-line: http://www.epa.gov/athens/publications/reports/EPA_600_R03_033.pdf.

Johnson, B. and A. Tuli, 2013. Soil Sampling And Dynamic Monitoring of Temperature, Soil Moisture, Humidity, and Pressure During Bedded Fumigant Applications or Broadcast Fumigant Applications. Protocl for study 285, Environmental Monitoring Branch. On-line: http://www.cdpr.ca.gov/docs/emon/pubs/protocol/study285protocol.pdf

Paperniek, S.K., S.R. Yates, and D.O. Chellimi. 2010. A Standardized Approach for Estimating the Permeability of Plastic Films to Soil Fumigants under Various Field and Environmental Conditions. J. Env. Qual, 40(5):1375-82. On-line: http://www.ars.usda.gov/SP2UserFiles/Place/20360500/pdf_pubs/P2359.pdf

Spurlock, F. 2013. Effect of Chloropicrin Application Practices on Cumulative and Maximum Chloropicrin Flux. Memorandum to R. Segawa, Envirnomental Monitoring Branch, DPR. On-line: http://www.cdpr.ca.gov/docs/emon/pubs/ehapreps/analysis_memos/2433-segawa_final.pdf

Spurlock, F. 2015. Variability in Simulated Chloropicrin and 1,3–dichloropropene Volatilization From Bare Ground Broadcast Applications. Memorandum to P. Wofford, Envirnomental Monitoring Branch, DPR. On-line: http://www.cdpr.ca.gov/docs/emon/pubs/ehapreps/analysis_memos/spurlock_hydrus.pdf

Spurlock, F., B. Johnson, A. Tuli, S. Gao, J. Tao, F. Sartori, R. Qin, D. Sullivan, M. Stanghellini and H. Ajwa. 2013. Simulation of Fumigant Transport and Volatilization from Tarped Broadcast Applications. Vadose Zone Journal. doi:10.2136/vzj2013.03.0056.

APPENDIX

Within field means and CV (coefficient of variation) for PIC and 13D PE and TIF simulations.
maxflux in ug m-2 sec-1, 100 lb/ac applied basis.

fumigant	tarp	depth	field	mean ER	mean maxflux	CVER	CVmaxflux
13D	PE	12	LH1	0.384	20.1	0.185	0.323
13D	PE	12	LH2	0.295	12.0	0.146	0.214
13D	PE	12	LH3	0.290	13.3	0.399	0.468
13D	PE	12	cro1	0.562	39.2	0.091	0.233
13D	PE	12	din1	0.656	49.5	0.052	0.192
13D	PE	12	din2	0.571	37.8	0.086	0.252
13D	PE	12	mer1	0.446	25.9	0.141	0.239
13D	PE	12	san1	0.512	33.2	0.133	0.226
13D	PE	12	sto1	0.486	29.1	0.066	0.105
13D	PE	12	sto2	0.386	21.5	0.285	0.434
13D	PE	12	vis1	0.475	28.8	0.259	0.486
13D	PE	12	wat1	0.369	18.4	0.265	0.438
13D	PE	12	wat2	0.522	35.8	0.154	0.382
13D	PE	12	wat3	0.398	21.3	0.175	0.300
13D	PE	12	wat4	0.495	30.9	0.062	0.093
13D	PE	18	LH1	0.216	8.4	0.358	0.303
13D	PE	18	LH2	0.112	4.8	0.199	0.247
13D	PE	18	LH3	0.124	5.1	0.452	0.505
13D	PE	18	cro1	0.392	16.7	0.147	0.240
13D	PE	18	din1	0.552	28.6	0.113	0.186
13D	PE	18	din2	0.456	20.2	0.144	0.285
13D	PE	18	mer1	0.275	10.8	0.230	0.259
13D	PE	18	san1	0.369	15.9	0.226	0.320
13D	PE	18	sto1	0.396	17.5	0.117	0.167
13D	PE	18	sto2	0.204	7.6	0.373	0.339
13D	PE	18	vis1	0.355	16.0	0.429	0.603
13D	PE	18	wat1	0.129	5.2	0.384	0.392
13D	PE	18	wat2	0.319	14.1	0.406	0.484
13D	PE	18	wat3	0.191	7.2	0.364	0.317
13D	PE	18	wat4	0.272	10.0	0.172	0.149
13D	TIF	12	LH1	0.121	4.9	0.140	0.148
13D	TIF	12	LH2	0.099	4.1	0.095	0.117
13D	TIF	12	LH3	0.096	3.9	0.284	0.410
13D	TIF	12	cro1	0.177	6.6	0.067	0.090
13D	TIF	12	din1	0.243	8.5	0.067	0.045
13D	TIF	12	din2	0.206	7.4	0.071	0.038
13D	TIF	12	mer1	0.138	5.4	0.120	0.108
13D	TIF	12	san1	0.158	6.2	0.132	0.113
13D	TIF	12	sto1	0.149	5.7	0.081	0.061
13D	TIF	12	sto2	0.120	5.0	0.226	0.278
13D	TIF	12	vis1	0.161	6.0	0.266	0.182
13D	TIF	12	wat1	0.118	4.9	0.208	0.237
13D	TIF	12	wat2	0.164	6.5	0.159	0.113
13D	TIF	12	wat3	0.128	5.3	0.142	0.143

fumigant	tarp	depth	field	mean ER	mean maxflux	CVER	CVmaxflux
13D	TIF	12	wat4	0.149	6.1	0.056	0.072
13D	TIF	18	LH1	0.082	2.2	0.252	0.407
13D	TIF	18	LH2	0.052	1.1	0.117	0.192
13D	TIF	18	LH3	0.054	1.2	0.314	0.441
13D	TIF	18	cro1	0.139	4.4	0.123	0.139
13D	TIF	18	din1	0.217	7.1	0.104	0.145
13D	TIF	18	din2	0.177	5.6	0.112	0.098
13D	TIF	18	mer1	0.099	2.9	0.188	0.277
13D	TIF	18	san1	0.127	4.2	0.206	0.225
13D	TIF	18	sto1	0.131	4.4	0.111	0.115
13D	TIF	18	sto2	0.077	2.2	0.269	0.411
13D	TIF	18	vis1	0.132	4.0	0.385	0.454
13D	TIF	18	wat1	0.057	1.2	0.266	0.405
13D	TIF	18	wat2	0.116	3.5	0.344	0.465
13D	TIF	18	wat3	0.076	2.0	0.253	0.421
13D	TIF	18	wat4	0.098	2.9	0.124	0.232
PIC	PE	12	LH1	0.259	14.1	0.159	0.188
PIC	PE	12	LH2	0.207	10.3	0.116	0.144
PIC	PE	12	LH3	0.202	10.8	0.356	0.293
PIC	PE	12	cro1	0.367	23.1	0.081	0.211
PIC	PE	12	din1	0.438	26.9	0.047	0.151
PIC	PE	12	din2	0.383	22.5	0.075	0.183
PIC	PE	12	mer1	0.295	16.4	0.126	0.173
PIC	PE	12	san1	0.335	20.3	0.122	0.188
PIC	PE	12	sto1	0.318	18.2	0.061	0.114
PIC	PE	12	sto2	0.260	14.9	0.252	0.297
PIC	PE	12	vis1	0.317	17.8	0.239	0.359
PIC	PE	12	wat1	0.254	13.8	0.238	0.278
PIC	PE	12	wat2	0.344	21.6	0.140	0.292
PIC	PE	12	wat3	0.271	14.9	0.151	0.202
PIC	PE	12	wat4	0.326	19.3	0.057	0.076
PIC	PE	18	LH1	0.161	11.3	0.296	0.188
PIC	PE	18	LH2	0.094	7.6	0.161	0.210
PIC	PE	18	LH3	0.100	7.6	0.415	0.454
PIC	PE	18	cro1	0.270	15.6	0.128	0.055
PIC	PE	18	din1	0.374	19.3	0.091	0.069
PIC	PE	18	din2	0.315	17.2	0.119	0.073
PIC	PE	18	mer1	0.198	13.3	0.195	0.091
PIC	PE	18	san1	0.254	13.9	0.199	0.128
PIC	PE	18	sto1	0.268	13.1	0.098	0.086
PIC	PE	18	sto2	0.153	10.5	0.321	0.280
PIC	PE	18	vis1	0.247	14.9	0.371	0.205
PIC	PE	18	wat1	0.105	8.0	0.327	0.314
PIC	PE	18	wat2	0.225	13.8	0.353	0.159
PIC	PE	18	wat3	0.146	10.4	0.304	0.240
PIC	PE	18	wat4	0.196	13.0	0.145	0.092
PIC	TIF	12	LH1	0.075	4.3	0.138	0.129

fumigant	tarp	depth	field	mean ER	mean maxflux	CVER	CVmaxflux
PIC	TIF	12	LH2	0.062	3.7	0.085	0.067
PIC	TIF	12	LH3	0.060	3.5	0.300	0.342
PIC	TIF	12	cro1	0.107	5.4	0.068	0.087
PIC	TIF	12	din1	0.140	6.6	0.043	0.039
PIC	TIF	12	din2	0.122	5.9	0.056	0.027
PIC	TIF	12	mer1	0.085	4.6	0.114	0.106
PIC	TIF	12	san1	0.097	5.2	0.118	0.102
PIC	TIF	12	sto1	0.091	4.8	0.059	0.050
PIC	TIF	12	sto2	0.076	4.5	0.228	0.233
PIC	TIF	12	vis1	0.096	4.9	0.229	0.162
PIC	TIF	12	wat1	0.075	4.4	0.215	0.213
PIC	TIF	12	wat2	0.100	5.4	0.143	0.082
PIC	TIF	12	wat3	0.080	4.6	0.137	0.116
PIC	TIF	12	wat4	0.094	5.3	0.050	0.070
PIC	TIF	18	LH1	0.049	2.2	0.255	0.336
PIC	TIF	18	LH2	0.031	1.1	0.113	0.190
PIC	TIF	18	LH3	0.033	1.3	0.321	0.443
PIC	TIF	18	cro1	0.083	3.7	0.120	0.097
PIC	TIF	18	din1	0.123	5.5	0.080	0.123
PIC	TIF	18	din2	0.103	4.6	0.092	0.081
PIC	TIF	18	mer1	0.060	2.7	0.190	0.171
PIC	TIF	18	san1	0.076	3.6	0.188	0.169
PIC	TIF	18	sto1	0.078	3.8	0.088	0.106
PIC	TIF	18	sto2	0.047	2.2	0.277	0.382
PIC	TIF	18	vis1	0.077	3.5	0.350	0.351
PIC	TIF	18	wat1	0.035	1.3	0.263	0.422
PIC	TIF	18	wat2	0.069	3.1	0.344	0.397
PIC	TIF	18	wat3	0.046	2.0	0.263	0.378
PIC	TIF	18	wat4	0.059	2.8	0.135	0.186